SEM AND HRTEM ANALYSIS OF CARBON NANOSTRUCTURES SYNTHESIZED WITH A NEW PULSED ELECTRIC ARC DISCHARGE TECHNIQUE

D. Saucedo-Jiménez[a], J. Ortiz-López[a], V. Garibay-Febles[b]*, and E. Palacios-González[b]

[a] Instituto Politécnico Nacional, Escuela Superior de Física y Matemáticas, Edificio 9 UPALM-Zacatenco, Departamento de Física, Av. Instituto Politécnico Nacional s/n, 07738, Mexico City, Mexico

[b] Instituto Mexicano del Petróleo, Laboratorio de Microscopia Electrónica de Ultra Alta Resolución, Eje Central Lázaro Cárdenas Norte 152, 07730, México City, Mexico

*Corresponding author, E-mail: vgaribay@imp.mx, phone 525591757608, Fax. 525591756380

Recibido: Febrero 2013. Aprobado: Abril 2013.
Publicado: Mayo 2013.

ABSTRACT

We propose and investigate a new method for the synthesis of carbon nanostructures by electric arc discharge, which consists of a sharp cathode and a rotating anode specially designed to create a discontinuous and periodic discharge over block-shaped compacted powders of catalytic mixture. With this design it is possible to control the pulse time width and frequency of discharge by variation of the size of the catalytic blocks and of the anode angular speed. This arrangement imposes important changes to conventional growth conditions of carbon nanostructures which are of central relevance in nucleation and growth models, such as the stability of the plasma jet plume, and gradients in temperature and in carbon concentration, among others. To illustrate the type of structures that can be obtained with this method we present some results under the following conditions: catalytic mixture of C (graphite), Ni, Co, Fe and S powders in 95/0.5/2.8/1.4/0.3 % molar fraction concentrations, respectively, 200 torr hydrogen atmosphere, 360 rpm anode angular velocity, 13.8 ms discharge pulse time width and 24 Hz pulse repetition rate. Under these conditions we are able to synthesize double wall carbon nanotubes. Other carbon nanostructures obtained under diverse preparation conditions are described. The synthesized structures are analyzed with scanning electron microscopy, transmission electron microscopy as well as with Raman spectroscopy.

Keywords: Carbon nanotubes, Double wall carbon nanotubes, Pulsed electric arc discharge, H_2 Arc Discharge

ANÁLISIS POR MICROSCOPIA ELECTRÓNICA DE BARRIDO Y TRANSMISIÓN DE ALTA RESOLUCIÓN PARA NANOESTRUCTURAS DE CARBONO SINTETIZADAS CON UNA NUEVA TÉCNICA DE DESCARGA DE ARCO PULSADA

RESUMEN

Proponemos investigar y un nuevo método para la síntesis de nanoestructuras de carbono por descarga de arco eléctrico, que consta de un cátodo agudo y un ánodo giratorio especialmente diseñados para crear una descarga discontinua y periódica sobre polvos compactados en forma bloque de mezcla catalítica. Con este diseño es posible controlar el intervalo de tiempo del pulso y frecuencia de la descarga por la variación del tamaño de los bloques catalíticos y de la velocidad angular del ánodo. Esta disposición impone cambios importantes en las condiciones de crecimiento convencionales de nanoestructuras de carbono que son de importancia central en modelos de nucleación y crecimiento, tales como la estabilidad de la pluma de plasma, gradientes de temperatura y concentración de carbono, entre otros. Para ilustrar el tipo de estructuras que se pueden obtener con este método se presentan algunos resultados en las siguientes condiciones: mezcla catalítica de C (grafito), Ni, Co, Fe y polvos S en 95/0.5/2.8/1.4/0.3% fracción molar, respectivamente, 200 torr atmósfera de hidrógeno, 360 rpm de velocidad angular del ánodo, 13,8 ms en intervalo de tiempo del pulso y 24 Hz frecuencia de repetición del pulso. Bajo estas condiciones, se puede sintetizar nanotubos de carbono de pared doble. Otras nanoestructuras de carbono se obtienen bajo diversas condiciones de preparación. Las estructuras sintetizadas se analizaron con microscopía electrónica de barrido microscopía, electrónica de transmisión, así como con la espectroscopia de Raman.

Palabras claves: Nanotubos de Carbono, Nanotubos de Carbono de Doble Pared, Descarga de Arco Eléctrico Pulsada.

INTRODUCTION

Y. Ando has recently reviewed carbon nanotube synthesis by the arc-discharge method [1, 2]. *Ando's* group introduced various modifications and improvements to the arc discharge technique, which are relevant to the present work. To increase the yield of SWNT production, they devised electrodes with a 30° angle inclination instead of the usual arrangement with electrodes facing each other at a 180° angle. Under this configuration the arc plasma between electrodes occurs in the form of a jet and they called this variation the 'arc plasma jet (APJ) method'. Single Wall Carbon Nanotubes (SWNTs) synthesized in this way look macroscopically as a black web-like material which appears distributed all around the reactor chamber. In the APJ method, SWNT growth occurs when carbon clusters and vaporized metal catalysts are both in flight, in a similar fashion as it occurs in the laser ablation method [3, 4, 5]. In both these techniques, the plasma produced by the local evaporation of metal-enriched graphite condenses in the form of SWNT, metal nanoparticles and amorphous carbon. *Ando's* group also advanced the use of hydrogen as buffer gas after first introduced by *Wang* et al [6]. Using hydrogen arc discharge and front facing electrodes (no catalysts added) they were able to synthesize multiwall carbon nanotubes (MWNT) with the thinnest innermost tube ever obtained of 0.3 nm diameter containing an atomic carbon linear chain inside it [3]. *Liu* et al [7, 8] combined both APJ and hydrogen arc discharge to devise a semi continuous method of high yield SWNT synthesis using a catalytic mixture of Ni, Co, Fe, FeS and graphite powders. With a somewhat similar experimental setup and composition of catalytic mixture, our group determined subtle anisotropies in carbon nanotube, *V. Alvarez* et al [9]. described the synthesis of SWNT inside a reactor under 200 torr of hydrogen gas with the so-called arc-plasma-jet method consisting of a sharp inclined cathode pointing towards a static anode provided with cavities filled with a catalytic mixture consisting of C (graphite), Ni, Co, Fe, and FeS powders. The most visible result of synthesis is a black web-like material formed by entangled ropes of long SWNTs hanging from objects and supports inside the reactor. A black and fluffy material largely made up of SWNTs is also deposited on the walls of the reactor.

Pulsed arc discharge techniques were first introduced in 1999 by *Sugai* et al. [10] for the synthesis of fullerenes and SWNTs. Their method was called 'high-temperature pulsed arc discharge (HTPAD) technique' in which an intermittent discharge between carbon electrodes was generated (with a pulsed high voltage power supply) inside a quartz tube placed in a cylindrical furnace operated at about 1000 °C using He, Ar or Kr as buffer gases. Their method was capable to produce pulse widths in the 0.05-30 ms range at repetition rates between 3 to 300 Hz. Temperature and current control in this technique allowed the synthesis of double wall carbon nanotubes (DWNTs) with an appropriate choice of catalysts [11]. Pulsed discharge can also be produced mechanically by bringing front-facing electrodes within a close distance and then moving them away from each other in periodic cycles. When electrodes are within few millimeters, arc discharge is triggered; when their separation is large enough, the discharge is extinguished. These techniques have been used to produce carbon nanostructures with intermittent arc discharge submerged in water with 5 ms pulse widths at 15-20 Hz repetition rates [12].

In this paper we describe a new method of carbon nanostructure synthesis by a mechanically driven pulsed arc discharge using a conveniently designed spinning anode. The only account found in the literature for the use of a rotating electrode (anode) involves continuous arc discharge [13], not pulsed operation as described in the present work.

The mechanisms by which carbon nanotubes nucleate and grow are still the subject of investigation. The VLS (vapour-liquid-solid) model proposed by *Saito* et al. in

1995 [14], proposes that carbon vapor and metallic particles generated by electric discharge or laser ablation condense and form liquid carbide particles. During cooling down, SWNTs begin to grow when carbon atoms are expelled from the carbon-supersaturated carbide particles. *Kataura* and collaborators [15] proposed a model for laser ablation synthesis. In their model carbon clusters condense with fullerene-like structures. Some of this carbon is dissolved in metal particles and when the metal particles are saturated with carbon; their surfaces become covered with fullerene-like fragments. These fragments are the seeds from which SWNTs grow.

In all these models, important aspects of nucleation and growth processes are involved: the heating and cooling rates generated by the discharge, the catalytic activity of the metal particles, the flow of carbon clusters and metallic particles (convection currents), the stability of the plasma, and the pressure of the buffer gas. Synthesized material in the conventional continuous electric arc discharge technique is predominantly composed of fullerenes or of carbon nanotubes depending on the pressure of the buffer gas. The use of alternating current arc discharge changes growth conditions and produce new kind of carbon structures as reported by *Zeng* et al [16]. In pulsed direct-current discharge, temperature and concentration gradients of atoms and clusters as well as cooling/heating conditions will change with time so that variations in the growth environment are expected to occur and affect the resulting synthesized material. A number of topologic defects may be introduced during growth that could result in novel carbon nanostructures.

It is the aim of this work to propose and investigate a new design of a pulsed hydrogen arc plasma jet technique in which conditions on nucleation and growth processes in carbon nanotubes may be controlled in an innovative fashion. Some representative results are presented to illustrate the effects of new growth conditions imposed by our technique.

MATERIALS AND METHODS

In the present work we introduce modifications to the method described by Alvarez et al. [9], with the use of a spinning anode whose design allows the generation of a pulsed electric discharge. The anode spin is driven by an electrical motor externally mounted to the reactor chamber. The discharge is established between an inclined sharpened cathode (6 mm diameter) of high purity graphite, and blocks of catalytic powder mixture assembled on a circular graphite disk anode (10 cm diameter). An annular channel (1 cm deep and 1.5 cm radial width) of mean radius R (3 cm) is carved in the anode disk to receive the catalytic powder mixture in different possible arrays.

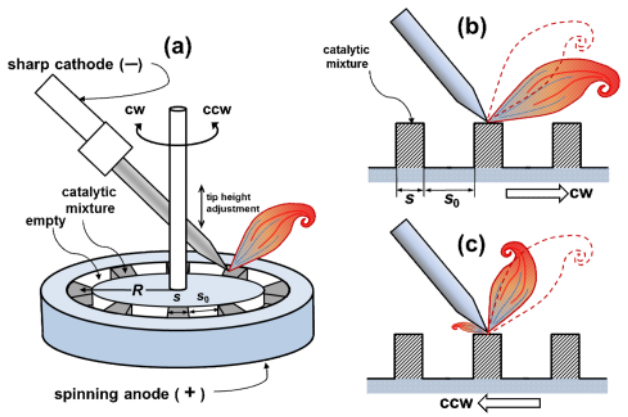

Fig.1. The option illustrated in Fig. 1(a) is to alternate blocks of catalytic mixture with empty sections inside the channel to generate a pulsed discharge with a time duration Δt which is proportional to the block width s and inversely proportional to the rotating speed ω.

The vertical position of the cathode tip is adjusted to trigger the electric discharge against the top of the catalytic blocks when their separation is of few millimeters. When the tip is above an empty section the discharge will shut down and discharge will be triggered again when the next block is brought below the cathode tip by the rotation of the anode disk. Several combinations of pulsed discharge times and pulse repetition rates can be envisaged by properly designing

the widths and distribution of catalytic blocks and empty sections along the channel.

Continuous discharge can also be implemented by filling up the whole channel with catalytic mixture as shown in Fig. 2.

For an anode rotating at constant speed ω (expressed in r.p.m.), designed with a uniform distribution of n catalytic blocks of width (arc length) s and n empty sectors of width (arc length) s_0, the discharge pulse time width Δt (in seconds) and the pulse repetition rate ν (in Hertz) are:

$$\Delta t = \frac{60}{2\pi}\frac{s}{R\,\omega} = \frac{60}{n\omega}\left(\frac{s}{s+s_0}\right); \qquad (1)$$

$$\nu = \frac{2\pi}{60}\frac{R\omega}{s+s_0} = \frac{n\omega}{60} = \left(\frac{s}{s+s_0}\right)\frac{1}{\Delta t}; \qquad (2)$$

The elapsed time (in seconds) between each discharge event will be

$$\Delta t_0 = \frac{60}{2\pi}\frac{s_0}{R\,\omega} = \frac{60}{n\omega}\left(\frac{s_0}{s+s_0}\right); \qquad (3)$$

The last expression in equation (2) establishes the dependence between pulse width Δt and repetition rate ν. This relation imposes a limit on the possible variations that can be applied on the variations of Δt and ν. With our system's arrangement and using a 2800 rpm electric motor we can in principle vary the pulse width in the range 0.57 ms ≤ Δt ≤ 194 ms and the repetition rate in the range 5 Hz ≤ ν ≤ 880 Hz.

The sense of rotation of the anode will have different effects on the plasma jet of the discharge as shown schematically in Figs. 1(b) and 1(c). Plasma jet with a static anode is outlined with dashed lines. With anode rotation, however, the jet will be 'pulled' along the sense of rotation when this is in the clockwise direction (cw). If, on the other hand, rotation is counterclockwise (ccw), the jet is 'pulled' in the opposite direction and a small jet will appear in the spinning direction behind the cathode tip as shown. This arrangement will impose important changes in the plasma jet and consequently on the growth conditions of carbon nanotubes and other structures.

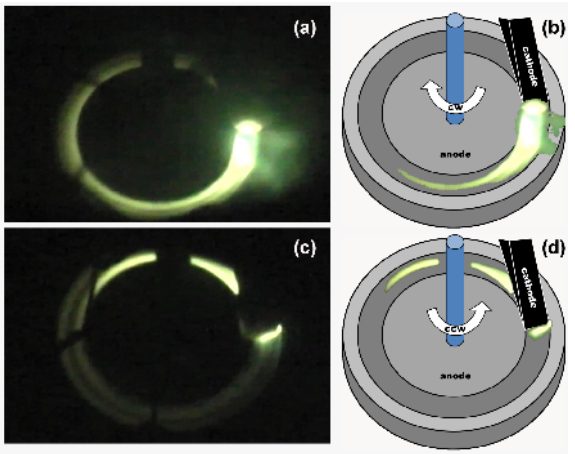

Fig. 2. Photographs of arc discharge for (a) clockwise (cw) and (c) counterclockwise (ccw) anode rotation. Plasma jet is seen with a very bright light emission. The stele of the anode hot spot left behind by the discharge is seen as a complete circle of weaker emission. Dark lines across these circles are shadows of a chicken wire net placed inside the reactor to capture carbon nanotubes in web-like form. Interpretation of photographs with line drawings are shown in (b) and (d) for cw and ccw rotation, respectively.

Fig. 2 show actual photographs of the arc discharge plasma jet for cw rotation (a) and ccw rotation (c) under continuous discharge conditions (annular channel completely filled with catalytic mixture). Line drawings in (b) and (d) are helpful for the interpretation of the photographs. Plasma jet is seen with a very bright light emission. The stele of the anode hot spot left behind by the discharge is seen as a complete circle of weaker emission. It can be seen how the plasma jet is affected by the spinning direction of the anode. In cw rotation, plasma jet is 'pulled ahead' the cathode tip as illustrated in Fig. 1(b), while in ccw rotation it is 'pulled behind' the cathode tip.

Synthesized material was analyzed with transmission electron microscopy (TEM) using a JEOL JEM-2200FS (200 kV) instrument. Scanning electron microscopy (SEM) was performed with a NOVA Nanolab DualBeam instrument. For Raman spectroscopy we used a Horiba Jobin Yvon LabRam HR800 instrument.

RESULTS AND DISCUSSION

Pulsed discharge characteristics under hydrogen atmosphere.

With the reactor filled with hydrogen gas at 200 torr, the discharge was triggered with 150A DC current supplied by a commercial 22.8 kVA electric welding station externally connected to the reactor chamber. The anode was designed with a block array having $n = 4$ filled and empty sectors with $s/s_0 = 0.5$ and the rotational speed was $\omega = 360$ rpm. Equations (1) and (2) yield $\Delta t \approx 13.8$ ms and $v \approx 24$ Hz for the discharge pulse time width and the pulse repetition rate, respectively. Under these conditions, the time elapsed between each discharge is $\Delta t_0 \approx 27.6$ ms. These conditions would correspond to the continuous ablation regime defined by Geohegan's group (pulses of the order of 10 ms at low repetition rates), which are advantageous for the growth of nanostructures other than SWNTs in the laser ablation technique [5].

An induction coil was wound around one of the current supply cables to monitor the pulsed DC arc discharge. The voltage waveform induced in the coil during discharge events was measured with a digital oscilloscope (Tektronix TDS 430A).

Fig. 3(a) shows the typical time dependence of the voltage signal at the sensor coil during a single discharge event for cw anode spinning. Signals for ccw spinning show analogous features. The discharge signal extends from 19.2 ms to 41.2 ms and consists of abrupt up and down swings of voltage. The integrated voltage signal in Fig. 3(b) is related to the negative of the discharge current (Faraday's Law) which shows a smoother behavior. Three regions in the time sequence of the discharge can be distinguished in both signals. Discharge ignition occurs (D1 in Fig. 3(c), blue shaded area in the 19-23 ms range) about 4 ms before the block's leading edge moves just below the cathode tip. Discharge extinction occurs (D2 in Fig. 3(c), blue shaded area in the 37-41 ms range) about 4 ms after the block´s trailing edge moves just below the tip. In the intermediate region (D in Fig. 3(c), yellow shaded area in the 23-37 ms range) the cathode tip is found above the block all along its geometrical thickness. The time width of the intermediate region is of ~14 ms, which agrees with $\Delta t \approx 13.8$ ms calculated with eq. (1) for the experimental conditions employed. From the above considerations we estimate that the critical distance between the block and the tip for discharge ignition and extinction is of about 4.6 mm.

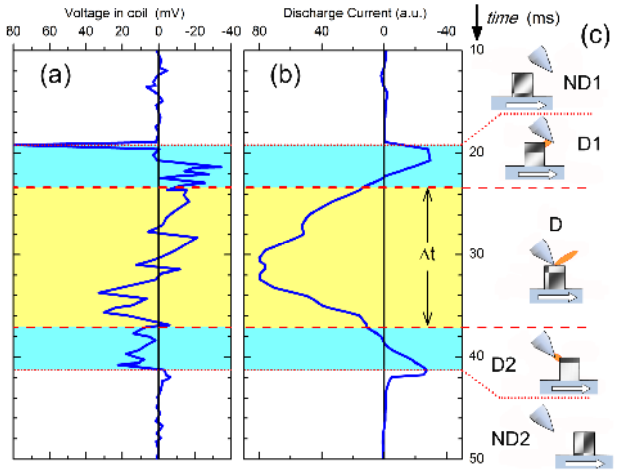

Fig. 3. Measurement of a single discharge event with an anode designed with n = 4 and s0/s = 2 rotating at 360 rpm in clockwise direction. Expected pulse width is Δt = 13.8 ms (shaded in yellow) at a repetition rate ν = 24 Hz. (a) Typical time dependence of the voltage signal at the sensor coil in the discharge event. The signal extends over the expected Δt because discharge starts and ends beyond the geometrical shape of the catalytic blocks (blue shaded areas). (b) Discharge current obtained as the negative of the integrated voltage signal. (c) Schematic illustration of sequence of events in discharge ignition and extinction: ND1, no discharge while the block is far away at the left of the tip; D1, discharge ignition when block is close to the left of the tip; D, discharge when block is directly below the tip; D2, discharge extinction when block is moving away to the right from the tip; ND2, no discharge while the block is far away to the right of the tip.

Synthesis of double-wall carbon nanotubes (DWNT)

As illustrative examples of the application of our technique, we present results and analysis of the material synthesized under ccw anode rotation under the conditions described above for anode design and

rotational speed (n = 4, s/s_0 = 0.5 and ω = 360 rpm). The molar fraction composition of the catalytic powder mixture was:

C(95%)/Ni(0.5%)/Fe(1.4%)/Co(2.8%)/S(0.3%)

which is similar to the one used by Li *et. al.* [17]. To assemble the catalytic blocks in the anode channel a binder must be used to agglomerate the powders. Two types of binders were tried: methyl cellulose and conductive carbon paint (SPI Supplies, Structure Probe, Inc.) and found best results with the first one. The analyzed specimens were taken from the web-like material that hangs inside the reactor after a synthesis session is performed.

Fig. 4 is a TEM image of a selected specimen of the synthesized material which illustrates the type of DWNTs obtained under the above experimental conditions. Experiments performed with different anode rotational speed (same anode design) indicate that DWNT production is sensitive to discharge repetition rate but we were not able to determine which is optimal in our system. In Fig 4(a) a DWNT of about 3 nm internal diameter is clearly seen to lie across the image from top left to bottom right. A magnification of the area marked by the yellow square in Fig. 4(a) is shown below in both (b) and (c). The amplified image is analyzed along the yellow lines cutting across the DWNT diameter with the software Digital Micrograph 3.7.0 (Gatan Inc., Pleasanton, CA, USA) which measures pixel intensity as a function of position along the chosen line length (bar plots at the right hand side). From pixel contrast it is clearly seen that the DWNT walls are double and separated by about 0.35 nm which agrees with the expected DWNT inter-wall distance.

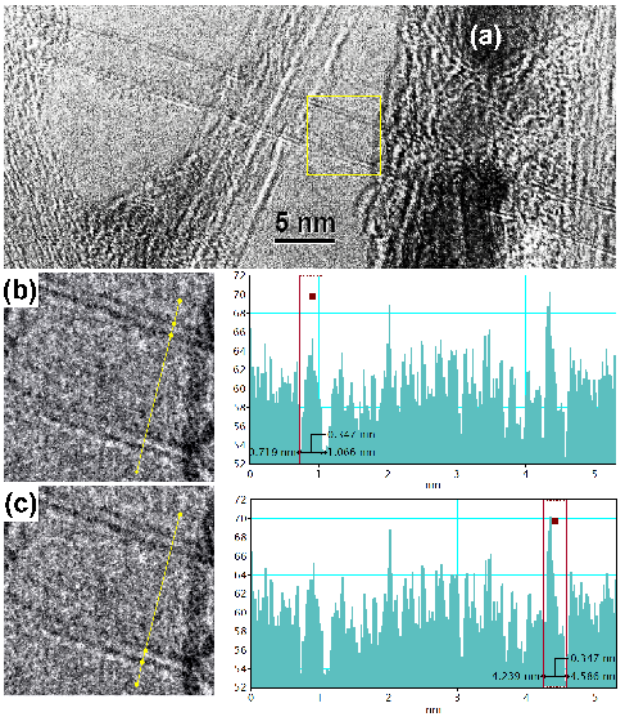

Fig. 4. (a) TEM image of a double wall carbon nanotube (DWNT) synthesized with our pulsed arc discharge technique. In (b) and (c) the zone enclosed by the yellow square in (a) is analyzed. (b) Left: analysis of amplified image along the yellow line. Right: Pixel intensities along that line show that the uppermost DWNT wall is formed by tubes with inter-wall distance of about 0.35 nm. (c) Similar analysis applied to the lower DWNT wall yields an inter-wall distance also of 0.35 nm. From (b) and (c) internal diameter of the DWNT is determined to be about 3.17 nm.

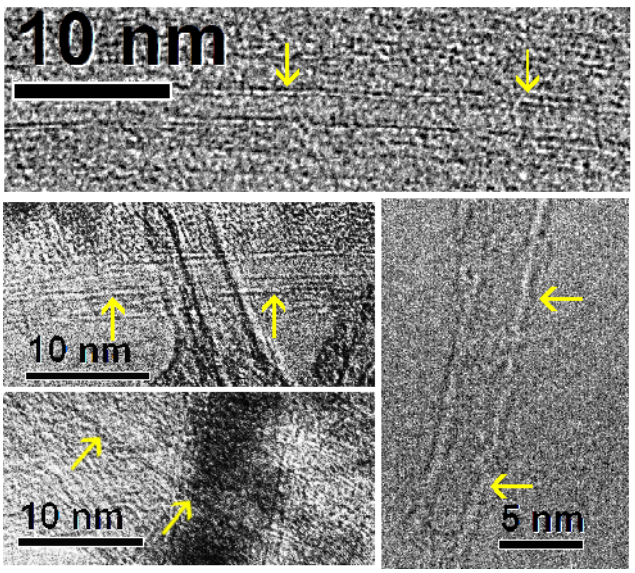

Fig. 5. TEM images of various synthesized DWNTs marked with yellow arrows. Internal diameters of observed DWNTs range from 1.3 to 3.2 nm.

The synthesized material is by no means homogeneous as can be seen in Fig. 4(a). Further TEM analysis showed also the presence single wall nanotubes (SWNTs), catalytic metal residues (both bare and covered with a layered envelope of graphitic carbon) and amorphous carbon.

A precise statistics of the analyzed images could not be performed but a rough estimate indicates that about 30±10% of the tubular structures are DWNTs of various diameters, the rest are SWNTs. Examples of other observed DWNTs (marked with yellow arrows) are shown in Fig. 5. Internal diameters of observed DWNTs range from 1.3 to 3.2 nm.

Fig. 6 displays representative Raman spectra under 633 nm excitation of the synthesized material. Radial breathing modes (RBM) in Fig. 6(a) can be fitted with 14 lorentzian peaks whose spectral positions and relative intensities are represented by the vertical segments below the spectrum. Of these peaks, 11 of them are consistent with the presence of DWNTs.

The diameter D (in nm) of a SWNT can be obtained with the relationship $D = 248/\nu_{RBM}$ [18] (see upper scale in Fig.6(a)) where ν_{RBM} (in cm^{-1}) is the Raman RBM resonant frequency of the SWNT. Assuming that RBM modes of SWNT components of a DWNT are independent [17, 19], the DWNT inter-wall distance d can be calculated as:

$d = (D_X - D_N)/2 = 124(1/\nu_X - 1/\nu_N)$, where D_X and D_N are the external (X) and internal (N) diameters of the SWNTs with corresponding RBM frequencies ν_X and ν_N, respectively. In Fig. 6(a), peaks compatible with the presence of DWNTs should be those for which $d = 0.35 \pm 0.02$ nm. Peaks marked with letter N in Fig. 6(a) are consistent with internal SWNT components of DWNTs and would correspond to diameters in the range from 0.84 nm to 1.51 nm. DWNTs of larger internal diameter (greater than 2.48 nm) would be located below 100 cm^{-1}, out of the measured spectral range. Corresponding external SWNTs components of DWNTs are marked with letter X. In summary, we find that the measured RBM signal is consistent with the presence of 5 different DWNT species.

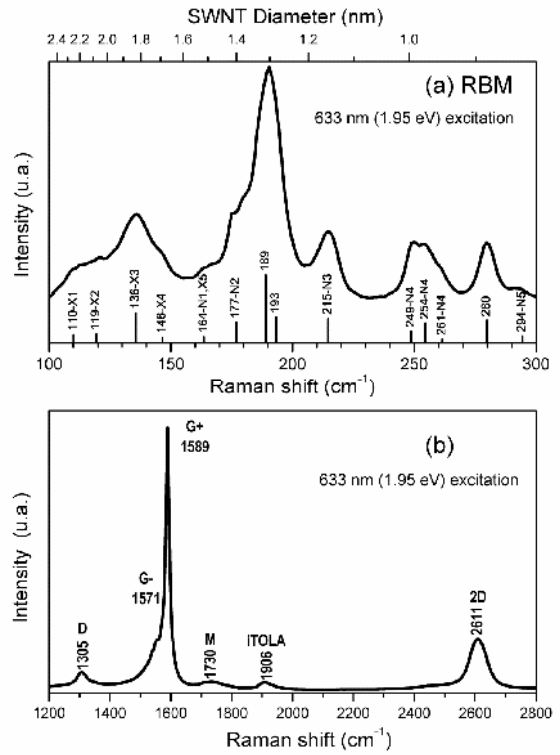

Fig. 6. Measured Raman spectra at 633 nm excitation. (a) RBM region showing positions in cm-1 of 14 lorentzian peaks that fit the spectrum. Peaks marked Xn and Nn are consistent with the presence of DWNTs, here n is a number that denotes correspondence between SWNT components of a DWNT. Peaks Xn are compatible to the external SWNT component while Nn is compatible to the internal component of a DWNT. (b) Raman spectra at higher frequency identifying D and G bands, M and 2D overtones, and iTOLA combination mode.

Raman response at higher frequencies above the RBM range is shown in Fig. 6(b). Typical bands characteristics of SWNTs are observed in the spectrum. The defect-induced D-band, located at 1305 cm^{-1}, is considerable weaker than the tangential mode G-band at 1589 cm^{-1}, indicating a good structural quality of SWNTs and DWNTs in our synthesized material. The G-band splits into two components G+, G-, typical of tangential modes in SWNTs (and DWNTs). Weaker bands, typical of sp^2 carbons and SWNTs, are observed at higher frequencies and assigned to the combination mode iTOLA at 1906

cm^{-1} and to overtone modes at 1730 cm^{-1} (M-band) and at 2611 cm^{-1} (2D-band or G'-band) [18].

Synthesis of other carbon nanostructures

Various carbon structures can be obtained under different preparation conditions with our system. One example is shown in the SEM image of Fig. 7. The image of Fig. 7(a) illustrates a carbon particle formed by graphene sheets in petal-like arrangement forming what has been called 'carbon nano-rose' [2, 20].

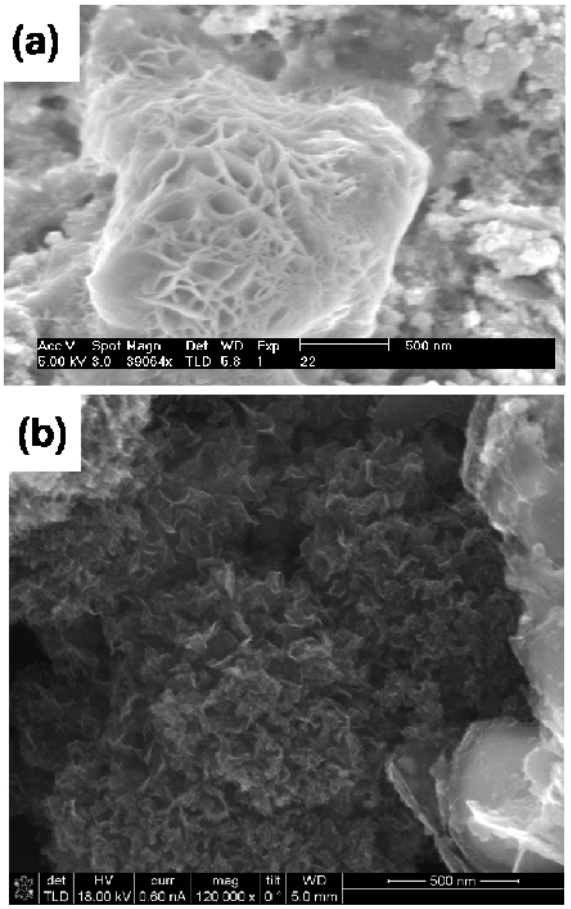

Fig. 7. (a) Carbon particle in the shape of a 'carbon nano rose' with petal-like sheets of graphene synthesized under discharge pulses of 3 ms at 173 Hz repetition rate; (b) Similar formations of graphene sheets collected from the anode obtained under pulsed discharge.

Interesting formations that resemble the so called 'carbon micro-trees' [21, 22] are shown in Fig. 8. In Fig. 8(a) peculiar hedgehog-like spike formations are observed in the SEM image taken of material collected from the anode. The spike average diameter is of about 80 nm and their tips in some instances appear to have hexagonal shape. Fig. 8(b) is another view of similar formations in the same sample prepared under 200 Torr hydrogen, with a catalytic mixture prepared with a significant larger molar content of sulfur: C (92.48)/Fe (1.41)/Ni (2.52)/S (2.91)/Co (0.68) and continuous discharge at 600 rpm ccw rotation speed.

Fig 8(c) illustrates another view of the spike formations in which EDX microanalysis was performed on the area indicated by the yellow square. The spectra in Fig. 8(d) shows the presence of catalytic metals Ni, Fe and Co, in addition to a considerable amount of sulfur (aluminum signal Al is due to sample holder).

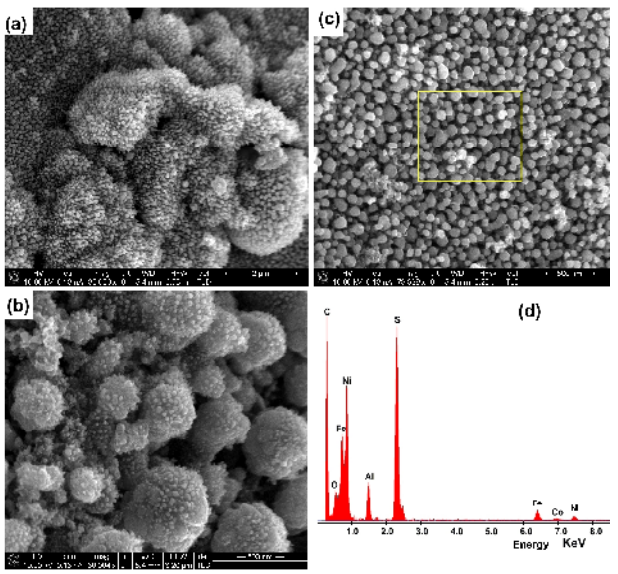

Fig. 8. (a) Hedgehog-like spike formations obtained under continuous discharge and high sulfur content in the catalytic mixture; (b) other formations observed in the same sample showing features similar to 'carbon micro-trees' [21, 22]; (c) another view of the spike formations for which EDX microanalysis was performed on the area indicated by the yellow square; (d) EDX microanalysis showing the presence of catalytic metals Ni, Fe and Co in addition to a considerable amount of sulfur (aluminum signal Al is due to the sample holder).

Elemental weight percent (wt%) quantification (corrected by subtracting Al signal) yields the composition

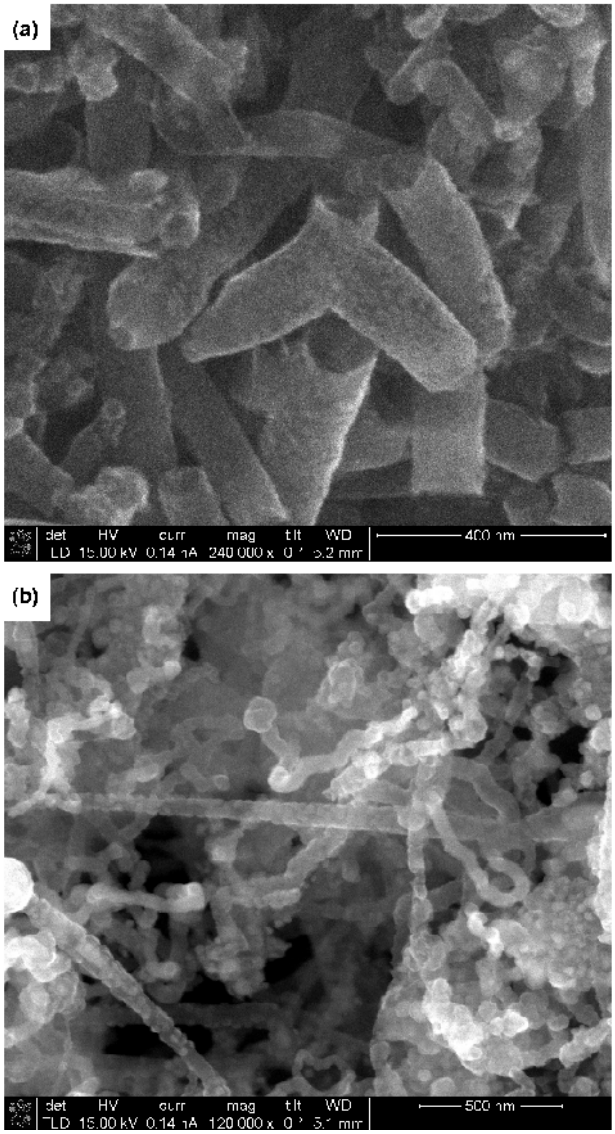

Fig. 9. Effects of increasing sulfur content in catalytic mixture: (a) SEM image of tubular formations with sulfur nodules decorating their sidewalls. A Y-junction is clearly seen in the image that grow as consequence of a carbon nanotube branching mechanism triggered by sulfur; (b) another view of the same sample.

C(48.43)/O(3.40)/Fe(17.40)/Ni(20.97)/S(8.86)/Co(0.94) which is equivalent to a molar fraction composition of 77.46/4.07/5.98/6.85/5.31/0.30 for the respective elements. No doubt that the higher sulfur content is responsible of the peculiar formations observed, as has been reported by several authors [23].

The presence of sulfur also promotes a branching mechanism in carbon nanotube growth [23]. As a consequence of this mechanism the appearance of Y-junctions, as the one shown in Fig 9(a), occur in samples prepared with increased sulfur content.

In this case, the sample was prepared from a molar composition C (93.84)/Fe (1.43)/Ni (2.56)/S (1.48)/Co (0.69), ccw rotation, pulsed discharge of 6 ms at 80 Hz and 100 Torr hydrogen pressure. Sidewalls of these nanotubes are seen to be decorated with sulfur nodules (as indicated by EDX) as can be seen in Fig. 9(b) for the same sample.

CONCLUSIONS

We have developed a simple and inexpensive novel system for the synthesis of carbon nanotubes and other carbon nanostructures by a pulsed arc discharge technique under hydrogen atmosphere. The novelty in the system is the use of a rotating anode which can be design with alternating empty and filled blocks of catalytic mixture. Our system was tested and was able to produce double wall carbon nanotubes and other type of interesting nanostructures. DWNTs were obtained under pulse widths and repetition rates that in the laser ablation technique promote the growth of nanostructures other than SWNTs. The developed system allows the variation of a great number of growth parameters which remain to be tested to fully take advantage of its capabilities. Particular choices of growth conditions in our system can produce, without any doubt, a new variety of carbon nanostructures.

ACKNOWLEDGMENTS

One of us (JOL) gratefully acknowledges support from CONACYT (Mexico) trough project No. 57262 and to SIP-IPN through projects No. 20090768, 20100849 and 20110544, and additionally to EDI-IPN and COFAA-IPN for support through academic fellowships. We would like to thank Centro de Nanociencias y Micro-Nanotecnologias of IPN for the use of their Raman equipment and to Luis A. Moreno for his help in obtaining Raman spectra.

REFERENCES

[1] Ando Y., Zhao X. (2006) "Synthesis of carbon nanotubes by arc-discharge method" *New Diamond and Frontier Carbon Technology* 16:123-137.

[2] Ando Y. (2010) "Carbon nanotube: "The Inside Story" *J. Nanoscience and Nanotechnology* 10: 3726–3738.

[3] Geohegan D.B., Schittenhelm H., Fan X., Pennycook S.J., Puretzky A.A., Guillorn M.A., Blom D. A., Joy D.C. (2001) "Condensed phase growth of single-wall carbon nanotubes from laser annealed nanoparticulates" *Appl. Phys. Lett*. 78, 3307-3310.

[4] Puretzky A.A., Schittenhelm H., Fan X., Lance M.J., Allard L.F. Jr., Geohegan D.B. (2002) "Investigations of single-wall carbon nanotube growth by time-restricted laser vaporization" *Phys. Rev. B*. 65: 245425, 1- 9.

[5] Puretzky A.A., Styers-Barnett D.J., Rouleau C.M., Hu H., Zhao B., Ivanov I.N., Geohegan D.B., (2008) "Cumulative and continuous laser vaporization synthesis of singlewall carbon nanotubes and nanohorns" *Appl. Phys. A*. 93:849 – 855.

[6] Wang X.K., Lin X.W., Dravid V.P., Ketterson J.B., Chang R.P.H. (1995) "Carbon nanotubes synthesized in a hydrogen arc discharge" *Appl. Phys. Lett*. 66:2430-2433.

[7] Liu C., Cong H.T., Li F., Tan P.H., Cheng H.M., Lu K., Zhou B.L. (1999) "Synthesis and hydrogen storage of carbon nanofibers and single walled carbon nanotubes" *Carbon* 37:1865-1868.

[8] Liu C., Hui-Ming Cheng, Cong H.T., Li F., Su G., Zhou B.L., Dresselhaus M. S., (2000) "Synthesis of macroscopically long ropes of well-aligned single-walled carbon nanotubes" *Advanced Materials* 12:1190-1192.

[9] Cruz Alvarez V., Ortiz López J., Mejía García C. (2005) "Anisotropies in carbon nanotube synthesis by the hydrogen arc plasma jet method" *Fullerenes, Nanotubes and Carbon Nanostructures* 13:299-311

[10] Sugai T., Omote H., Shinohara H. (1999) "Production of fullerenes by high-temperature pulsed arc discharge" *Eur. J. Phys. D*. 9:369-372.

[11] Sugai T., Yoshida H., Shimada T., Okazaki T., Shinohara H. (2003) "New Synthesis of High-Quality Double-Walled Carbon Nanotubes by High-Temperature Pulsed Arc Discharge" *Nano Letters* 3(6):169 – 173.

[12] Imasaka K., Kanatake Y., Ohshiro Y., Suehiro J., Hara M. (2006) "Production of carbon nanoonions and nanotubes using an intermittent arc discharge in water" *Thin Solid Films* 506-507: 250–254.

[13] Bae J.C., Yoon Y.J., Lee S.J., Moon Song K.M., Baik H.K. (2002) "Diameter control of single-walled carbon nanotubes by plasma rotating electrode process" *Carbon* 40:2905–2911.

[14] Saito Y. (1995) "Nanoparticles and filled nanocapsules" *Carbon* 33:979-988.

[15] Kataura H., Kumazawa Y., Maniwa Y., Ohtsuka Y., Sen R., Suzuki S., Achiba Y. (2000) "Diameter control of single-walled carbon nanotubes" *Carbon* 38:1691 – 1697.

[16] Zeng H., Zhu L., Hao G., Sheng R. (1998) "Synthesis of various forms of carbon nanotubes by AC arc discharge" *Carbon* 36:259 – 261.

[17] Li L., Li F., Liu C., Cheng Hui-Ming (2005) "Synthesis and characterization of double-walled carbon nanotubes from multi-walled carbon nanotubes by hydrogen-arc discharge" *Carbon* 43:623 - 629.

[18] Dresselhaus M.S., Dresselhaus G., Saito R., Jorio A. (2005) "Raman spectroscopy of carbon nanotubes" *Physics Reports* 409:47-99.

[19] Dresselhaus M.S., Jorio A., Hofmann M., Dresselhaus G., Saito R. (2010) "Perspectives on carbon nanotubes and graphene raman spectroscopy" *Nano Lett.* 10:751- 758.

[20] Ando Y., Zhao X., Ohkohchi M. (1997) "Production of petal-like graphite sheets by hydrogen arc discharge" *Carbon* 35:153-158.

[21] Ajayan P.M., Nugent J.M., Siegel R.W, Wei B., Kohler-Redlich Ph. (2000) "Growth of carbon micro-trees" *Nature* 404:243.

[22] Jung Y.J., Wei B., Nugent J., Ajayan P.M. (2001) "Controlling growth of carbon microtrees" *Carbon* 39: 2195-2201.

[23] Romo-Herrera J.M., Sumpter B.G., Cullen D.A., Terrones H., Cruz-Silva E., Smith D.J., Meunier V., Terrones M. (2008) "An Atomistic Branching Mechanism for Carbon Nanotubes: Sulfur as the Triggering Agent" *Chem. Int. Ed*. 47:2948-2953.